Communications

Primary Particle Melting Rates and Equiaxed Grain Nucleation

Q. HAN and A. HELLAWELL

This article is concerned with the survival of a relatively dilute dispersion of small solid particles (*e.g.*, 20 μm) in a large bath of liquid, at temperatures above the liquidus temperature of some alloy system. The situation has obvious relevance to castings of clean alloy melts (*i.e.*, those having no heterogeneous sites for nucleation, as might be created by grain refining additions), where the nucleation of equiaxed grains can be promoted only by intrinsic particles of the primary solid phase—such as those which formed at chill surfaces and became detached or were produced by fragmentation of developing dendrites. The precise sources of such solid fragments are not of immediate concern here (for more information on these, see, *e.g.*, References 1 through 5) and we consider only how long such fragments are likely to survive in a thermally or solutally hostile environment. In practice, it is well known that casting with a very small superheat will result almost entirely in a fine equiaxed grain structure: Chalmers[6] termed this situation "big bang" nucleation. With large superheats, it is also well known that the grain structure of a "clean" alloy casting will probably be entirely columnar. The purpose of this article is to point out that there must be a sharp transition in the melting rate of primary phase particles with melt superheat, from a solutally controlled dissolution regime at low to moderate superheats, to a much more rapid melting regime at higher temperatures, where the particles melt without necessary compositional adjustment. This "thermosolutal" or melting-dissolving transition is demonstrated by some simple experiments with the transparent material, succinonitrile ($[CH_2CN]_2$ or "SCN"), and some comments are made on its possible relevance to foundry practice.

Refer to the schematic phase diagrams of Figures 1(a) and (b), without/with significant solid solubility, *i.e.*, solid-liquid distribution coefficients $k_0 = 0$ and $k_0 > 0$. Consider a dispersion of small spherical particles of radius $r \approx 10$ μm, such as spheroidized dendrite fragments, in a large volume of liquid of composition C_0, initially in equilibrium at temperature T_0. Taking case 1(a), we consider what happens if the temperature is raised to T_L, where $T_0 < T_L < T_M$, when all particles should melt. In a thermally isolated, adiabatic system, the heat required to melt the solid dispersion will cool the liquid by ΔT_m. An estimate of ΔT_m is necessary to assess its importance. We obtain ΔT_m by equating the solid and liquid volumes with the latent heat of fusion, ΔH, and the specific heat of the liquid, c_L; thus,

$$N_{P/V} \cdot 4/3\pi r^3 \Delta H = c_L \Delta T_m \qquad [1]$$

where $N_{P/V}$ = number of particles of radius r, per unit volume. Taking $N_{P/V} = 10^9$ m^{-3} (1 mm^{-3}) and $r = 10^{-5}$ m, any alloy system will suffice; thus, for δ-iron, $\Delta H \approx 2{\cdot}10^9$ J·m^{-3} and $c_L = 5.74{\cdot}10^6$ J·m^{-3} K^{-1}, yielding $\Delta T_m = 1.4{\cdot}10^{-3}$ K. The result is similar for materials of similar entropies of fusion. For the purposes of this discussion, we will assume that this is a negligible cooling effect and that such a large relative liquid volume may be regarded as remaining effectively isothermal. Even with an increase in particle density of two orders of magnitude, the effect would still be unimportant.

Within the temperature range $T_0 < T_L < T_M$ (Figure 1(a)), *i.e.*, up to the melting point of the solvent component, the melting rate is controlled by solvent/solute diffusion in the liquid, away from/toward the melting particle(s). Above T_M, the solid inevitably melts without time for significant material transport, as a pocket of pure solvent, and composition adjustment follows. This is where there is a thermosolutal transition in the melting rate. With significant solid solubility, Figure 1(b), disregarding solid diffusion (but see subsequent discussion), the corresponding transition temperature is the liquidus temperature where the solid melts without composition change, *i.e.*, at k_0C_0, and is given for any liquid composition, C_0, by

$$T_{T/S} = T_M - m_L k_0 C_0 \qquad [2]$$

where m_L is the liquidus slope. The locus of the thermosolutal temperature, $T_{T/S}$, is shown by the broken line in Figure 1(b).

Such dispersed particles of solid are generally moving about in the bulk liquid, and their melting causes local convection from thermal and solutal gradients so that thermal and solutal diffusion occur within limited boundary layers, δ_T and δ_S (these are not necessarily equal or constant). Simple linear melting rates can be expressed.

Above T_M in Figure 1(a) and $T_{T/S}$ in Figure 1(b), the solid melts without composition change by supply of latent heat, ΔH, through the boundary layer of mean thickness δ_T and the thermally controlled melting rate, v_H, rises from zero at T_M or $T_{T/S}$, with the superheat ΔT_+:

$$v_H \Delta H = \frac{k_L \cdot \Delta T_+}{\delta_T} \qquad [3]$$

where k_L is the thermal conductivity of the liquid.

Below T_M or $T_{T/S}$, the solutally controlled melting rate, v_S, rises from zero at the initial equilibrium temperature, T_0, to a maximum at T_M or $T_{T/S}$. For the case of negligible solid solubility, (Figure 1(a)) the rate is obtained from the solvent concentration profile of Figure 2(a), assuming steady-state liquid diffusion through a given solutal boundary layer, δ_S, giving

$$v_S = -\frac{D_L (C_L - C_0)}{(1 - C_0)\bar{\delta}_S} \qquad [4]$$

where D_L is the liquid diffusion coefficient and the concentrations are as indicated in Figure 2(a). With solid solubility (Figure 1(b)), the situation would, in principle, require some solid diffusion, as the equilibrium, interfacial, solid solvent composition at some temperature T_L ($<T_{T/S}$) would be at $k_0C_L > k_0C_0$, as in Figures 1(b) and 2(b). This would imply that the melting rate would be slightly reduced by solid diffusion but increased by the smaller composition

Q. HAN, Postdoctoral Research Fellow, is with the Materials Department, Oxford University, Oxford OX1 3PH, United Kingdom. A. HELLAWELL, Emeritus Research Professor, is with the Department of Metallurgy and Materials Engineering, Michigan Technological University, Houghton, MI 49931.

Manuscript submitted July 16, 1996.

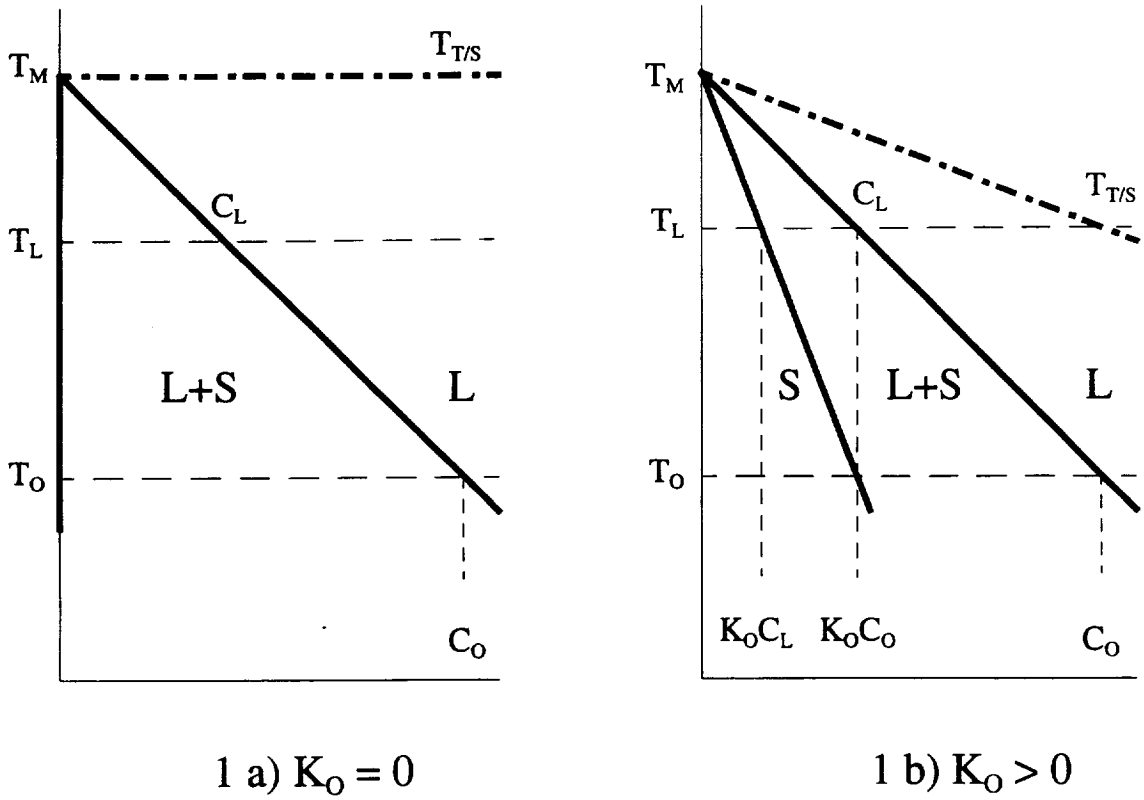

Fig. 1—Schematic phase diagrams (*a*) with negligible solid solubility, $k_o \rightarrow 0$, and *b* with significant solid solubility, $k_o >> 0$. C_o = liquid bath composition, and C_L = liquidus composition at some temperature, T_L, where T_M or $T_{TS} > T_L > T_o$. The heavy broken lines correspond to the thermosolutal transition in melting-dissolution kinetics.

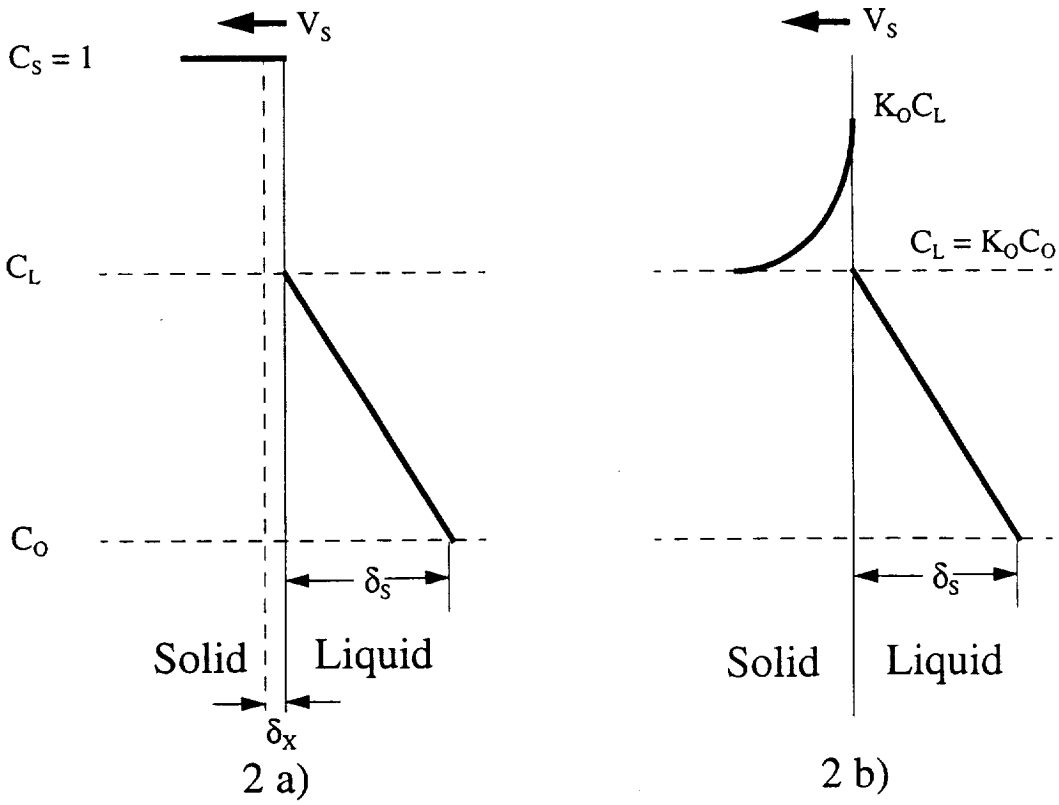

Fig. 2—(*a*) and (*b*) Schematic linear composition profiles for melting rates, $v_S = dx/dt$, controlled by diffusion through a boundary layer of thickness δ_S, corresponding to Figs. 1(a) and (b). Compositions are for *solvent* concentrations. With solid solubility, Fig. 1(b), there will be limited solid diffusion between interfacial and initial compositions, k_oC_L and k_oC_o.

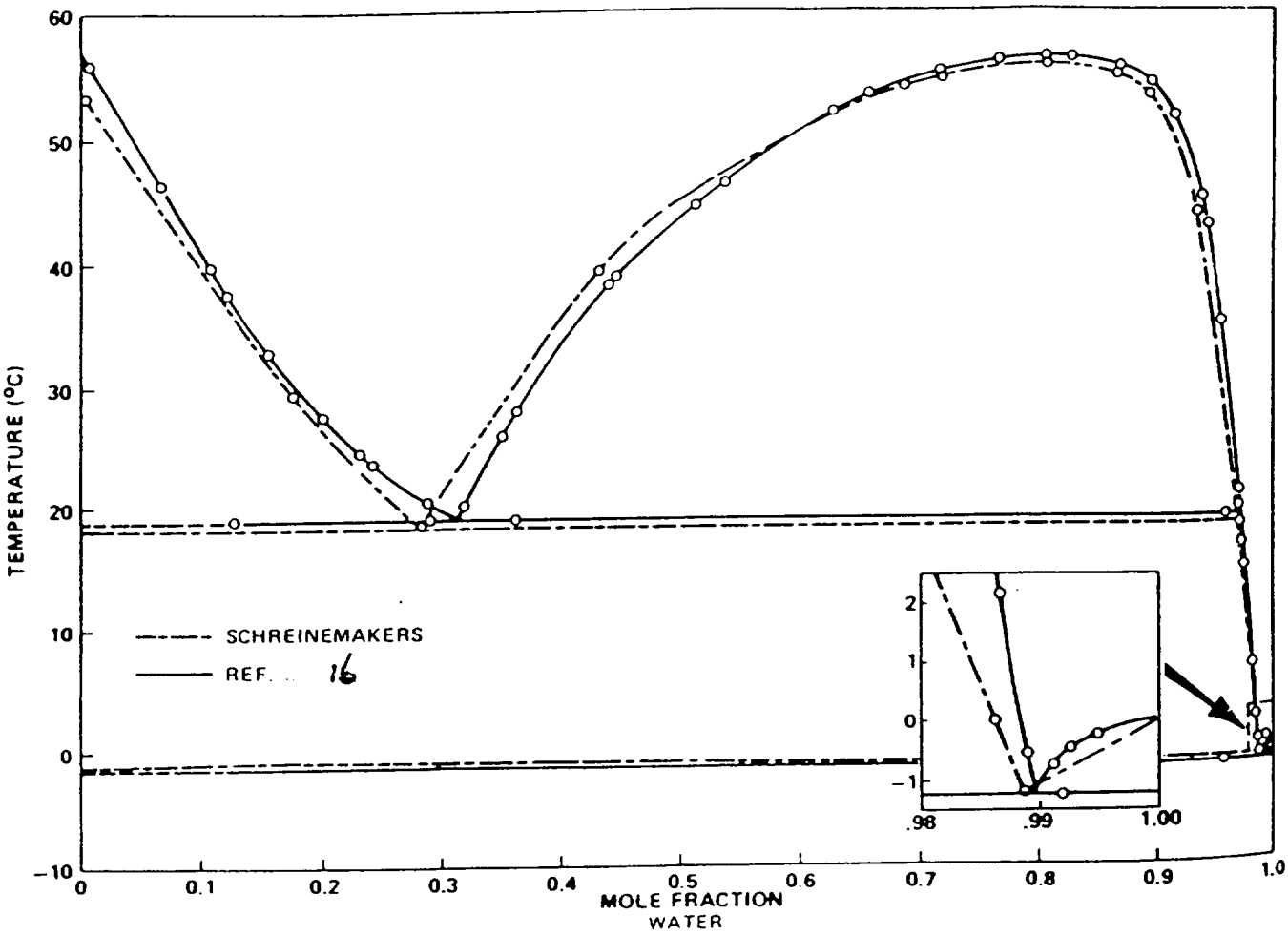

Fig. 3—The phase diagram, SCN-H_2O.[16] Referring to Fig. 1(a), $C_0 \approx 70$ pct molar SCN.

difference between solid and liquid, *i.e.*, $C_0 (1 - k_0)$, giving

$$v_S C_0 (1 - k_0) = -D_L \left(\frac{dC}{dx}\right)_L + D_S \left(\frac{dC}{dx}\right)_S \qquad [5]$$

where D_S is the solid diffusion coefficient. However, with D_L exceeding D_S by some two or three orders of magnitude and with a limited boundary layer, $\bar{\delta}_S$, the melting rates are generally sufficiently rapid (*e.g.*, 1 to 5 μm s^{-1}) for solid diffusion to be neglected in the present simplified context for small particles.

To confirm the expected transition in melting rate, simple, somewhat crude experiments were made with the transparent material, SCN ($[CH_2CN]_2$). The melting point of pure SCN is 58 °C[7]; the commercially pure material used in these experiments melted between 55 °C to 56 °C, as measured with a mercury/glass thermometer. Average melting rates were obtained by measuring the times taken to dissolve pellets of SCN in an aqueous solution, C_0, of monotectic composition (Figure 3) at ~0.3 mol pct H_2O/~9 wt pct H_2O, melting at ≈19 °C. There is negligible solid solubility so that Figures 1(a) and 2(a) are applicable.

Pieces of SCN weighing $\sim 10^{-1}$ g were rolled into spherical pellets of radius $r \approx 2.75$ mm. The liquid solution was contained in a test tube of 20-mm diameter and 100-mm height, which was placed in a water bath, the temperature of which could be controlled to within ±0.2 K. Pellets were dropped onto a wire mesh platform and observed through a telescope to measure the times to melt/dissolve at ambient temperatures between 35 °C to 65 °C. Liquid SCN is slightly more dense than the monotectic liquid, so that melting took place with slow convective mixing. In

Table I. Melting Times, t, and Mean Melting Rates, $\bar{v}_M$, for SCN in Aqueous Solution of Monotectic Composition (Figure 3)

Temperature (°C)	Time (s)	Mean Rates (μm s^{-1})
65.0	40	68.75
65.0	43	63.95
61.0	48	57.29
60.5	71	38.73
58.5	80	34.38
57.5	85	32.35
57.0	190	14.47
56.0	630	4.37
55.0	660	4.17
54.0	660	4.17
53.0	660	4.17
52.0	720	3.82
51.0	900	3.05
35.0	~2700 (est)	~1.00

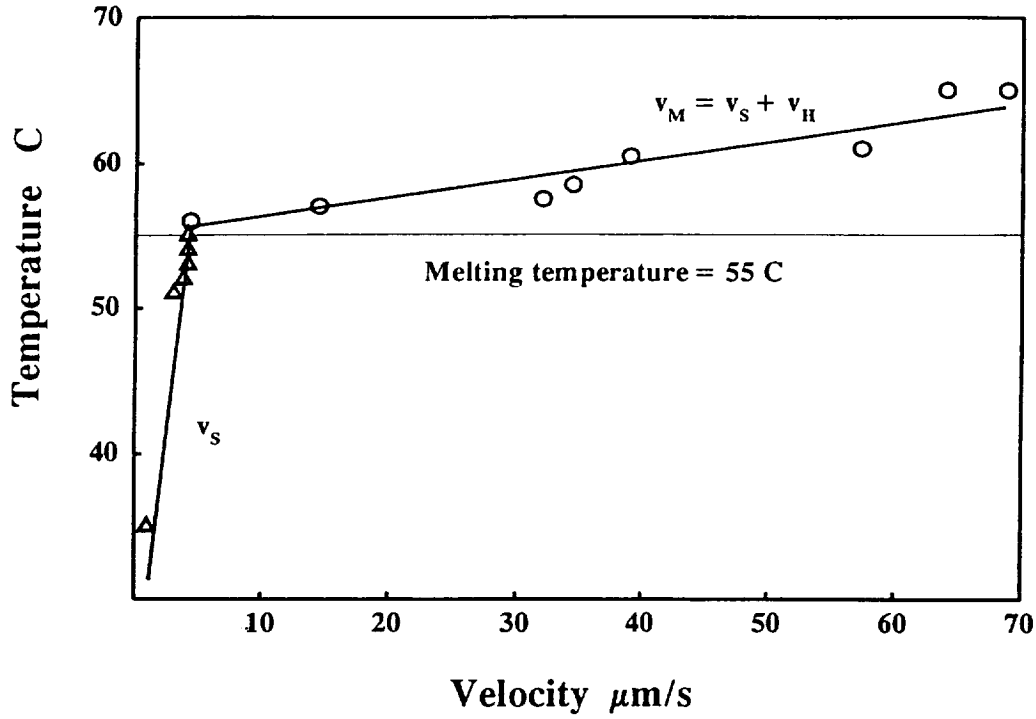

Fig. 4—Data from Table I, to illustrate an abrupt transition in melting rate at the melting point of impure SCN (55 °C). Δ—solutally controlled dissolution, and ○—thermally controlled melting.

Table I are listed the times, t, to melt/dissolve *vs* temperature, with derived mean melting rates, $\bar{v}_M = r/t$ in μm s^{-1}, which are plotted *vs* temperature in Figure 4.

As may be seen, the solutally controlled melting rates rise within a small range to ≈4.5 μm s^{-1} at $T_M \approx 55$ °C, and then thermally controlled melting takes over with an order of magnitude increase within 1 to 2 K of superheat.

Above the melting point, T_M, the melting rate $\bar{v}_M = \bar{v}_S + \bar{v}_H$, so that at some small superheat, ΔT_+, $\bar{v}_H = \bar{v}_S$. It was of interest to equate these rates from the simple expressions of Eqs. [3] and [4] assuming that $\bar{\delta}_T \approx \bar{\delta}_S$ (for want of a more rigorous approach). Taking ΔH for SCN = $5 \cdot 10^7$ J·m^{-3}, $k_L = 0.223$ W·m^{-1} K^{-1}[17] for liquid SCN, and $D_L \approx 3 \cdot 10^{-9}$ m^2 s^{-1} yields a value for $\Delta T_+ \approx 0.2$ K for $\bar{v}_H = \bar{v}_S$. Considering the gross simplications and crudity of the experiments, this seemed to be a very acceptable estimate compared with measurements. Also, taking the measured value of $\bar{v}_S$ at T_M, Eq. [4] yields a boundary layer thickness, $\bar{\delta}_S \approx 0.6$ mm, which is a credible estimate, compatible with visual inspection of convection around a melting pellet.

Other experiments were made which gave similar qualitative results. Thus, with pellets sitting at the bottom of the test tube, convection was greatly reduced and solutal melting rates were slower by ≈1/3 to ≈1/5, although they still showed the same abrupt increase to similar rates above T_M. Experiments with dissolution in pure water also showed the same step increase at T_M, but were complicated by the presence of two immiscible liquids (see phase diagram, Figure 3) and were therefore discounted.

A transition in the melting/dissolution rate of primary phase particles has been identified and confirmed experimentally. The existence of this thermosolutal transition seems to be rather obvious, but although there is extensive literature (*e.g.*, References 8 and 9) concerned with the dissolution and reaction rates of relatively massive additions to metal melts, as in steelmaking practice, there does not seem to have been attention given to the problem of small primary particles, which, having some relevance to foundry practice, may be worth discussion.

There is also extensive literature concerned with the effects of thermosolutal convection on dissolution rates, relevant to oceanographic and geological contexts, the melting of icebergs and reactions in magma chambers, with laboratory experiments conducted in various configurations (*e.g.*, References 10 through 12). These also include analyses of dissolution through boundary layers, but across wide areas, over long times, where the scales involved are some five to eight orders of magnitude greater than those of interest here. Of particular relevance, however, is an article by Woods,[13] which clearly recognizes and analyzes the difference between thermally controlled melting and solutally controlled dissolution; we were pleased to have confirmed this distinction experimentally.

What is implied (*e.g.*, Figure 1(a) or (b)) is that if molten alloy is poured at temperatures above T_M or T_{TIS}, any solid particles which nucleate on chill surfaces (as of a gating system) and become detached will have a negligible chance of survival before they can be swept into a mold. If poured below the transition temperature, the survival times of such fragments must always be significantly greater, although still short, *e.g.*, <5 seconds, and to function as sources of equiaxed grains, they would need to reach a position at/below the liquidus temperature within a brief time interval.

An order of magnitude estimate for fragment survival times might be made for small particles, *e.g.*, $r \approx 10$ μm, with some assumed boundary layer thickness, $\bar{\delta}_S \approx 20$ μm (an arbitrary guess). Thus, for Al − 4 wt pct Cu, $k_0 = 0.14$,

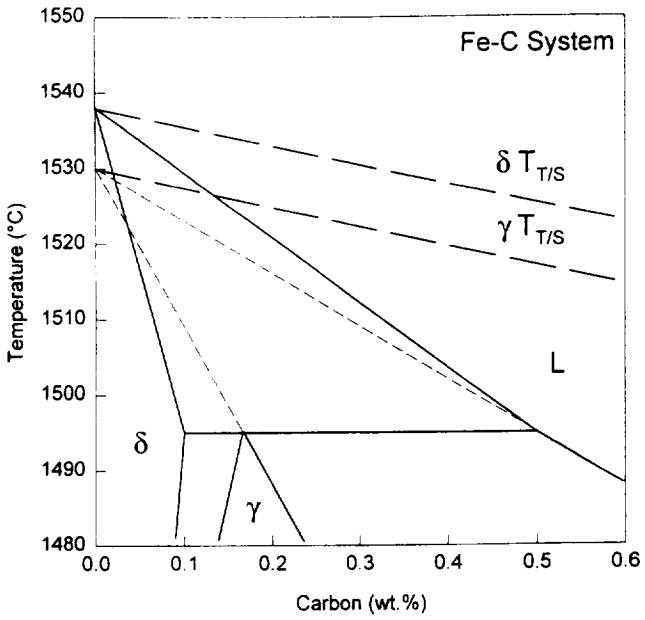

Fig. 5—The iron-carbon phase diagram around the peritectic region with the γ liquidus/solidus extrapolated to a hypothetical melting point of 1530 °C, and the thermosolutal transition temperatures $T_{T/S}$ for γ and δ iron from Eq. [2]. $T_{T/S} = T_M - m_L k_0 C_0$.

m_L = 2.6 K·wt pct^{-1}, T_M = 660.4 °C, and the liquidus temperature ≈650 °C. From Eq. [2], the thermosolutal melting transition should be at ≈659 °C and linear solutal melting rates can be estimated from Eq. [4]. Such linear estimates yield solutal melting rates from $\bar{v}_S \approx 2$ μm s^{-1} at 651 °C up to ≈17 μm s^{-1} at $T_{T/S}$ = 659 °C, or, assuming constant solution rates for the spherical particles, survival times falling from 5 to 0.6 seconds. Of course, with spherical geometry, the melting will accelerate as the particle shrinks, so these are optimistic survival estimates—for the arbitrary value of $\bar{\delta}_S$. In practice, for a shrinking submicron particle, the boundary layer probably also becomes negligible, so that the final radial melting or dissolving rate will tend to infinity.

However, if these estimates are of the correct order, the conclusion would be that very few fragments, introduced during the pouring/gating of a conventional casting, would be likely to survive long enough to grow into equiaxed grains, and, by implication, that only those evolving from a mushy zone, at later times and at lower temperatures, need be considered as potential embryo grains.

One case may be more relevant to such brief survival times, namely, the production of (Al base) rheocast billets using electromagnetic stirring (*e.g.*, Reference 14). In these configurations, the stirring rates are very rapid, ~1 m s^{-1}, within limited volumes (0.1 m), over small temperature ranges (<5 K), so that crystal fragments detached at a cooler position would circulate within times ≈10^{-1} s and therefore may well survive long enough to grow into grains.[15]

The case of steels across the δ/γ peritectic range offers some opportunity for speculation. Referring to the binary Fe-C phase diagram (Figure 5) for δ-iron, $m_L \approx 72$ K wt pct C^{-1} and $k_0 = 0.17$; for γ-iron, $m_L \approx 60$ K·wt pct C^{-1} and $k_0 \approx 0.35$. The melting transition temperature, $T_{T/S}$, from the previous argument (Figure 1(b)) would be as shown for the δ and γ phases. For a melt composition of 0.2 wt pct C, $T_{T/S}$ for γ would lie about 10 K lower than that for δ and only about 2 K above the δ liquidus. Thus, as might be anticipated, any solid which nucleated at a chill position below the peritectic temperature as γ-iron would have a much shorter survival probability than a similar fragment of δ-iron. For small, isolated, single-crystal fragments in liquid, it seems probable that there might be considerable hysteresis in the δ/γ transformation, both on cooling and heating. There are too many unknown factors (*e.g.*, solid liquid surface energies and temperature fluctuations in a pour/gating operation) to offer any realistic estimates for such survival times in the present article, but it is suggested that there may be a matter here for further consideration. As in rheocastings, the use of similar electromagnetic stirring in the continuous casting of steel will also serve to transport detached dendrite fragments very rapidly from hot to colder positions where they may survive and grow. This may account, in part, for the finer equiaxed structures which such stirring promotes, as compared with unstirred castings where slower natural convection operates.

This work was part of a program concerned with the grain structure of castings, supported by the National Science Foundation, under Grant Nos. DMR-92-06783 and DMR-95-21875, and The National Aeronautics and Space Administration, through NASA–Lewis Research Center, Contract No. NAG-3-1462.

REFERENCES

1. K.A. Jackson, J.D. Hunt, D.R. Uhlmann, and T.P. Seward: *Trans. TMS-AIME*, 1966, vol. 236, pp. 149-60.
2. T.F. Bower and M.C. Flemmings: *Trans. TMS-AIME*, 1967, vol. 237, pp. 1620-27.
3. M.E. Glicksman and R.J. Schaefer: *The Solidification of Metals*, Iron and Steel Institute, London, 1968, Book 110, pp. 43-48.
4. G. Hansen, A. Hellawell, S.Z. Lu, and R.S. Steube: *Metall. Mater. Trans. A*, 1996, vol. 27A, pp. 569-81.
5. J. Pilling and A. Hellawell: *Metall. Mater. Trans.*, 1996, vol. 27A, pp. 229-32.
6. B. Chalmers: *J. Aus. Inst. Met.*, 1963, vol. 8, pp. 255-60.
7. W. Kurz and D.J. Fisher: *Fundamentals of Solidification*, Trans Tech Publications, Aedermannsdorf, Switzerland, 1984, Appendix 12, p. 240.
8. R.I.H. Guthrie: *Engineering in Process Metallurgy*, Oxford University Press, Oxford, England, 1992.
9. T. Engh: *Principles of Metal Refining*, Oxford University Press, Oxford, England, 1992.
10. H.E. Huppert and J.S. Turner: *J. Fluid Mech.*, 1980, vol. 100, pp. 367-84.
11. D. Fang and A. Hellawell: *J. Cryst. Growth*, 1988, vol. 92, pp. 364-70.
12. R.C. Kerr: *J. Fluid Mech.*, 1994, vol. 280, pp. 255-85 and 287-302.
13. A.W. Woods: *J. Fluid Mech.*, 1992, vol. 239, pp. 429-48.
14. S. Blais, W. Loué, and C. Pluchon: *Proceedings of 4th Int. Conf. on Semi-Solid Processing of Alloys and Composites*, eds. E.H. Kirkwood and P. Kapranos, University of Sheffield, England, 1996, pp. 187-92.
15. A. Hellawell: *4th Int. Conf. on Semi-Solid Processing of Alloys and Composites*, Sheffield, England, 1996, pp. 60-65.
16. W.F. Kaukler and D.O. Frazier: *J. Cryst. Growth*, 1985, vol. 71, pp. 340-45.